Earth Surface Processes and Landforms, Volume 44, Issue 13, October 2019, pp. 2587-2599
DOI:10.1002/esp.4682

Temporal variation in suspended sediment transport: linking sediment sources and hydro-meteorological drivers

Kim Vercruysse[1,2], Robert C. Grabowski[1]

[1] Cranfield Water Science Institute, School of Water, Energy and Environment. Cranfield University, MK43 0AL, United Kingdom

[2] School of Civil Engineering, University of Leeds, Leeds LS2 9JT, United Kingdom.

Abstract

Suspended sediment concentrations (SSC) in rivers are variable in time due to interacting soil erosion and sediment transport processes. While many hydro-meteorological variables are correlated to suspended sediment concentrations, interpretation of these correlations in terms of driving processes requires in-depth knowledge of the catchment. Detailed sediment source information is needed to establish the causal linkages between driving processes and variations in SSC. This study innovatively combined sediment fingerprinting with multivariate statistical analyses of hydro-meteorological data to investigate how differential contributions of sediment sources control SSC in response to hydro-meteorological variables during high-flow events in rivers. Applied to the River Aire (UK), five sediment sources were classified: grassland topsoil in three lithological areas (limestone, millstone grit and coal measures), eroding riverbanks, and street dust. A total of 159 suspended sediment samples were collected during 14 high-flow events (2015-2017). Results show substantial variation in sediment sources during high-flow events. Limestone grassland and street dust, the dominant contributors to the suspended sediment, show temporal variations consistent with variations in total SSC, and are correlated with precipitation and discharge shortly prior and during high-flow events (i.e. fast mobilisation to and within river). Contrarily, contributions from millstone and coals grassland appear to be driven by antecedent hydro-meteorological conditions (i.e. lag-time between soil erosion and sediment delivery). Riverbank material is poorly correlated to hydro-meteorological variables, possibly due to weak source discrimination or the infrequent nature of its delivery to the channel. Differences in source-specific drivers and process interactions for sediment transport demonstrate the difficulty in generalising sediment transport patterns and developing targeted suspended sediment management strategies. While more research is essential to address different uncertainties emerging from the approach, the study demonstrates how empirical data on sediment monitoring, fingerprinting, and hydro-meteorology can be combined and analysed to better understand sediment connectivity and the factors controlling SSC.

Key words: Sediment fingerprinting, DRIFTS, hysteresis, sediment connectivity

Introduction

Natural suspended sediment (SS) transport dynamics in rivers are often strongly disturbed, especially when the degree of human intervention in a river catchment is high (Lexartza-Artza and Wainwright, 2011; Taylor and Owens, 2009; Walling et al., 2003b; Wohl, 2015), leading to problems such as excessive siltation, pollution, and ecosystem degradation (Bilotta and Brazier, 2008; Mauad et al., 2015). Sustainable management solutions require a comprehensive understanding of catchment erosion and sediment transport dynamics (Owens et al., 2005). However, high spatiotemporal variability in SS transport complicates our ability to quantify SS concentrations (SSC) and sources over multiple timescales (Bilotta et al., 2012; Vercruysse et al., 2017).

Past research has identified a range of hydro-meteorological variables (e.g. discharge, antecedent soil moisture conditions, rainfall intensity and duration, and air temperature) to explain (and predict) variations in SSC (Francke et al., 2014; Onderka et al., 2012; Perks et al., 2015; Tena et al., 2014; Zeiger and Hubbart, 2016; Zimmermann et al., 2012). However, variation in SSC is also driven by short- and long-term changes in sediment sources due to exhaustion in sediment supply, vegetation changes, mass movements, or human landscape disturbances (e.g. land cover change or dam construction) (Belmont et al., 2011; Grabowski and Gurnell, 2016; Rovira et al., 2015; Vanmaercke et al., 2016). These changes in sediment sources are only included implicitly into correlations between SSC with hydro-meteorological variables, which therefore only offer a partial explanation for the spatiotemporal variation in SS transport without actual information on the continuum of SS sources and transfer across the catchment (Bracken et al., 2015).

For example, the most commonly used hydro-meteorological explanatory variable for SSC is river discharge, and temporal variations (i.e. hysteresis patterns) in the sediment ratings curve (i.e. relationship between river discharge and SSC) are frequently used to extrapolate information about processes controlling SS availability, transport and sources (e.g. Aich et al., 2014; Eder et al., 2010; Francke et al., 2008; Lloyd et al., 2016; Pietroń et al., 2015; Sherriff et al., 2016; Smith and Dragovich, 2009; Sun et al., 2015; Williams, 1989). A clockwise hysteresis pattern during a high-flow event (i.e. when the peak SSC precedes the peak discharge) is typically attributed to contribution of sediment sources located close the river (Aich et al., 2014; Eder et al., 2010). Conversely, a counter-clockwise pattern, characterised by a delayed peak SSC relative to discharge, is attributed generally to contribution of more distant sediment sources becoming connected to the river system (Fan et al., 2012; Fang et al., 2015; Francke et al., 2014; De Girolamo et al., 2015; Tena et al., 2014). However, interpretation of hysteresis patterns in terms of processes and sediment sources strongly depends on the study site; similar variations in SSC can be the result of changes in the total sediment supply (e.g. exhaustion of all sediment sources) or changes in a sediment source (e.g. river bank collapse), which can only be determined by in-depth knowledge of the catchment (Smith and Dragovich, 2009; Vercruysse et al., 2017).

To improve the scientific understanding of the process interactions controlling SSC in rivers, empirical and analytical approaches are needed that differentiate sediment sources, quantify their contribution to the total SSC, and link them to hydro-meteorological drivers (Fryirs, 2013). In other words, alongside quantification of the

amount and timing of SS transport in rivers, there is a need for scientific data on sources of SS and how it changes over time, during and between high-flow events and over longer time spans.

To this end, many studies have investigated SS sources through sediment fingerprinting (e.g. Chen et al., 2016; Franz et al., 2014; Palazón et al., 2015; Tiecher et al., 2016; Vale et al., 2016), which has evolved significantly over the past decades as a method to estimate sediment source contributions directly from river sediment (Davis and Fox, 2009; Mukundan et al., 2012; Owens et al., 2016; Pulley and Collins, 2018). Particularly interesting from a monitoring perspective is the recent development of methods based on infrared spectrometry (Cooper et al., 2014a; Poulenard et al., 2009; Tiecher et al., 2016), which are more time- and cost-effective compared to traditional geochemical sediment fingerprinting methods (Collins et al., 2017). These advancements enable sediment fingerprinting to be easier applied at a finer temporal frequency (i.e. event scale) to retrieve detailed information on variations in SS sources.

Especially with the growing availability of detailed monitoring data in river catchments (e.g. discharge and precipitation), opportunities emerge to combine SS monitoring with sediment fingerprinting and multivariate analyses at fine temporal resolutions. Therefore, this study innovatively combines SS data with sediment fingerprinting and hydro-meteorological information to investigate how differential contributions of sediment sources control total SSCs in response to hydro-meteorological variables during high-flow events in rivers. Diffuse Reflectance Infrared Fourier Transform spectrometry (DRIFTS)-based sediment fingerprinting is applied on an extensive SSC dataset for the River Aire (UK) and combined with multivariate analyses of detailed

hydro-meteorological data to identify controlling factors and processes for source-specific SS transport dynamics. Better insights into these factors will help the development of source-specific erosion and sediment transport models, and guide targeted soil conservation and pollution prevention strategies (Owens et al., 2005; Perks et al., 2017; SedNet, 2009).

Materials and methods

Study area

The total catchment area of the River Aire is 879 km^2, with an area of 690 km^2 upstream of the point of SS sampling in the City of Leeds. Between 1989 and 2017, the mean annual rainfall was 1018 mm $year^{-1}$, and the mean discharge 15 $m^3 s^{-1}$. Based on random monthly SS measurements (i.e. manual samples taken on a random day each month) from the Environment Agency (EA) of England (1990-2014), the mean SSC in the River Aire within the city centre of Leeds is 15.8 mg L^{-1} (range: 0-100 mg L-1). The median absolute particle size of the SS ranges between 5.2 and 13.3 µm (Carter et al., 2006; Walling et al., 2003a).

The dominant land use is grassland (59%), followed by urbanised area (25%). The remaining land is covered in moorland (12%), primarily found at higher elevations in the upper catchment, and scattered arable land (4%). The catchment consists mainly of poorly draining loamy and clayey soils, with raw oligo-fibrous peats, and stagnohumic and stagnogley soils in the upper part, and brown earths and pelo-stagnogley soils in the middle and lower parts (Carter et al., 2003). The geology of the catchment dates from the Carboniferous Period and consists of three main zones:

Coal Measures (31%), Millstone Grit (46%), and limestone and shale formations (23%) (British Geological Survey, 2016) (Figure 1).

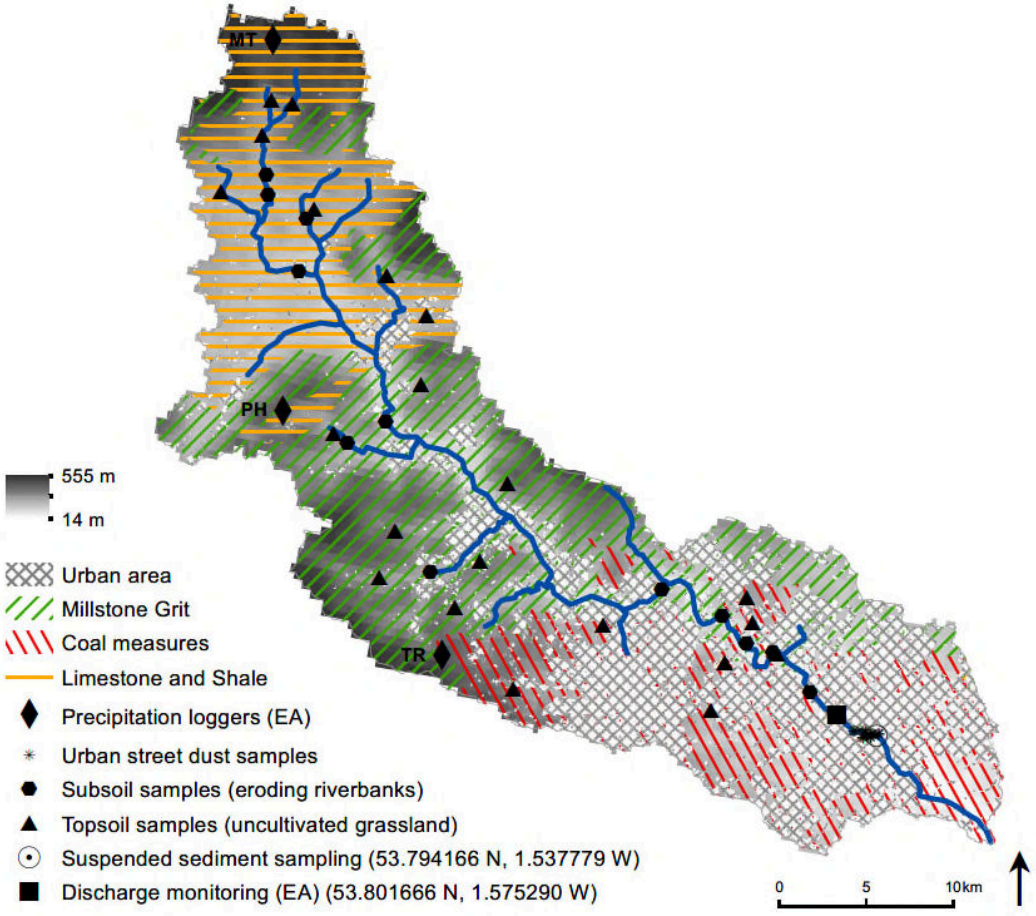

Figure 1: Catchment of the River Aire with sediment source areas and sampling locations (TR: Thornton Reservoir, PH: Proctor Heights, MT: Malham Tarn)

Suspended sediment and hydro-meteorological data

SS samples were collected with a depth-integrating SS sampler (type US DH-81) during individual high-flow events between June 2015 and March 2017. Due to the urban environment and frequent boat navigation at the sampling location, it was impossible to install an automated sampler in the river. Therefore, samples were

collected manually during daylight hours before, during, and after rainfall events with a frequency between 30 minutes and 2 hours, informed by real-time updates on river levels (https://www.gaugemap.co.uk) to capture discharge peaks. Water samples were filtered on pre-weighted, quartz fibre filters and dried for 2 hours at 105˚C (Cooper et al., 2014a; Pulley et al., 2015). In total, 14 high-flow events were sampled (159 individual samples), covering a range of peak discharges (23 to 120 $m^3 s^{-1}$) and peak SSCs (18 to 1000 mg L^{-1}) (Figure 1).

High-frequency (15-min) discharge and precipitation measurements were obtained from the EA. Discharge measurements originate from a monitoring station at Armley located 3 km upstream of the SS sampling site. Precipitation data were obtained from rain gauges located at the upstream edge of each geological zone at Malham Tarn (MT), Thornton Reservoir (TR), and Proctor Heights (PH) (Figure 1).

Sediment source data

Based on land use in the River Aire catchment and a previous sediment fingerprinting study (Carter et al., 2003), five potential SS sources were classified: soil from grassland in three geological zones (limestone (“L”), millstone grit (“M”), and coal measures (“C”)), eroding riverbanks (“R”) and urban street dust (“U”).

An erosion map based on the Revised Universal Soil Loss Equation (RUSLE) was used as a guideline during sampling to target zones within the catchment that are most prone to soil erosion. A total of 117 sediment source samples were collected. At each soil sampling location three subsamples were taken within one square meter. Source materials from grassland topsoil (21 locations x 3 replicates) and subsoil from eroding channel banks (12 locations x 3 replicates) were collected using a trowel (Figure 1).

The top 5 cm of the topsoil was sampled to ensure that only material likely to be eroded and transported to the river was collected (Carter et al., 2003; Cooper et al., 2014a; Martínez-Carreras et al., 2010; Pulley et al., 2015). Street dust samples (18 samples) were collected along road drains using a dustpan and brush (Cooper et al., 2014a; Pulley et al., 2015).

All sediment source samples were processed following the method developed by Poulenard et al. (2009). First, the samples were mixed with demineralised water and placed in a sonic bath for seven minutes to disaggregate clasts. Then the samples were wet sieved to retain the < 63 µm fraction to reduce the effect of particle size variations on source attribution and spectral distortion (Laceby et al., 2017; Poulenard et al., 2009). Finally, all source samples were also filtered on quartz fibre filters and oven-dried for two hours at 105˚C (Cooper et al., 2014a; Pulley et al., 2015).

Sediment fingerprinting

The DRIFTS-based sediment fingerprinting applied in this study is described in detail by Vercruysse et al. (2018). In summary, the method consists of three main steps: (i) measuring SS and sediment source samples with DRIFTS; (ii) testing whether source samples can be discriminated from each other based on their DRIFTS spectra through a discriminant analysis; and (iii) developing source-specific Partial Least Squares regression (PLSR) models based on DRIFTS spectra of experimental mixtures (54 mixtures; Vercruysse and Grabowski (2018)) with known source-quantities, which can subsequently be applied to estimate SS source contributions from DRIFTS spectra of SS.

The discriminant analysis demonstrated that urban street dust and material from grassland topsoil in the three lithological areas can be discriminated well based on their DRIFTS spectra, while riverbank has a lower degree of discriminatory power (Vercruysse and Grabowski, 2018). The difference in discriminatory power can be attributed to the primary origin of the sources. Riverbank material is generally a mixture of floodplain deposits consisting of various primary sediment sources, while street dust originates from distinctly different anthropogenic and natural sources (e.g. weathering of car tires, atmospheric deposition, road construction works) (Taylor and Owens, 2009; Vercruysse and Grabowski, 2018). The differences in discriminatory power are subsequently reflected in the uncertainty associated to the source-specific PLSR models, whereby the 95% confidence intervals range from ±10% for urban street dust and coals grassland, ±12-13% for limestone and millstone grassland, and ±18% for riverbank material (Table 1, supplementary material).

As the method is based on individual, source-specific PLSR models instead of a mass balance equation as in traditional sediment fingerprinting methods (Walling, 2013), the sum of all estimated source contributions is not set to 100%. In previous sediment fingerprinting studies using DRIFTS (Poulenard et al., 2009, 2012), a sum of these individually estimated contributions close to 100% was then considered an indication that all major sources were correctly identified. However, due to model uncertainties associated with the source-specific PLSR models, it is uncertain to what extent a deviation from 100% is caused by these uncertainties, by the sources included into the model, or by other factors such as particle size effects or changes in the DRIFTS spectra over time (i.e. non-conservancy) (Laceby et al., 2017). To address the

uncertainty related to the number of sources, Vercruysse et al. (2018) performed a sensitivity analysis of the PLSR model results by omitting individual sources from the source classification. The results demonstrate that when an important source (in terms of contribution) is omitted, more contribution is attributed to the least well-discriminated source (i.e. riverbank material), while estimated contributions of well-discriminated sources remain constant. Estimated contributions from riverbanks are therefore highly uncertain, as additional (unclassified) sources might still be captured within this group. However, the analysis also suggests that the part represented by the riverbank samples is an important source; omitting the riverbank as a source impacts significantly on the estimated contributions of other sources (Vercruysse and Grabowski 2018). Therefore, riverbank was retained as a potential source, but the high confidence intervals should be kept in consideration.

Table 1: Partial Least Squares regression model statistics (CI: confidence interval). Adopted from Vercruysse et al. (2018)

Model	R^2	95% CI
Limestone PLSR	0.884	± 12%
Millstone PLSR	0.877	± 13%
Coals PLSR	0.929	± 10%
Riverbank PLSR	0.790	± 18%
Urban PLSR	0.772	± 10%

Variation in suspended sediment sources

(i) Inter-event variation

Inter-event variation in SS transport is often observed (Alexandrov et al., 2007; Gao et al., 2013; Sherriff et al., 2016). It is expected that this inter-event variation in total SSC is also expressed in varying SS sources (Legout et al., 2013). Therefore, SS source contributions and hydro-meteorological variables were compared at the inter-

event scale. The event-based variables included total and source-specific SSCs (SSC_t (total), SSC_L, SSC_M, SSC_C, SSC_R, and SSC_U) together with discharge (Q) and antecedent precipitation totals (as a proxy variable for antecedent soil moisture conditions) for one day, 7 days and 21 days prior to the event (P_{1d}, P_{7d}, P_{21d}) (e.g. Perks et al., 2015; Seeger et al., 2004).

(iii) Intra-event variation

To gain insights into the intra-event variation in SS sources, hysteresis patterns between discharge and (source-specific) SSCs were visually examined to investigate possible changes in the dominant SS source throughout individual events, and to assess the consistency of source-specific hysteresis patterns (i.e. to assess whether source-specific SSCs vary simultaneously throughout events).

Hydro-meteorological drivers

A multivariate analysis was preformed to investigate the correlation between total SSC and source-specific SSCs with a range of hydro-meteorological variables in order gain insights into drivers and processes controlling temporal variation in SS sources and how these variations relate to variations in the total SSC. The multivariate dataset included all sampled SSCs, estimated source-specific SSCs, discharge and precipitation at the time of sampling (Q and P), as well as 1, 7 and 21 day antecedent discharge (Q_{1d}, Q_{7d}, Q_{21d}) and precipitation (P_{1d}, P_{7d}, P_{21d}) for the 3 monitoring stations (MT, PH and TR) (Figure 1).

Two types of multivariate analyses were done, each aimed at investigating a different level of correlation between the variables. First, a Pearson correlation analysis was performed to investigate pairwise correlations between SSC, source specific SSCs,

and hydro-meteorological variables. Second, relationships were established between SSC and source-specific SSCs (Y_i), and hydro-meteorological variables (X) to investigate whether SSC could be predicted based on these explanatory variables. To avoid selection of variables based on collinearity, PLSR was used. Compared to multiple linear regression, PLSR is better able to handle data with collinear and numerous explanatory variables (Karaman et al., 2013; Martens and Martens, 2000). Essentially, PLSR works similarly to principal component analysis (PCA), as it reduces a dataset with many variables (X; 14) and numerous measurements (observations; 159) into a few components by maximizing the covariance between the X and Y datasets (Wold et al., 2001).

In total, six SSC-PLSR models (i.e. one for the total SSC and five for the source-specific SSCs) were developed analogous to the approach described by Poulenard et al. (2009). The sum of squared PLSR loadings (SSL) were used as a measure to evaluate which hydro-meteorological variables define the model components (Karaman et al., 2013; Martens and Martens, 2000; Wold et al., 2001).

Results

Dominant suspended sediment sources

Limestone grassland was identified as the dominant SS source (average: 45% ± 12%), followed by urban street dust (average: 43% ± 10%) (Figure 2). Millstone and coals grassland contributed on average 19% (± 13%) and 14% (±10%) respectively, while eroding riverbanks accounted for 16% (± 18%) of the total SSC.

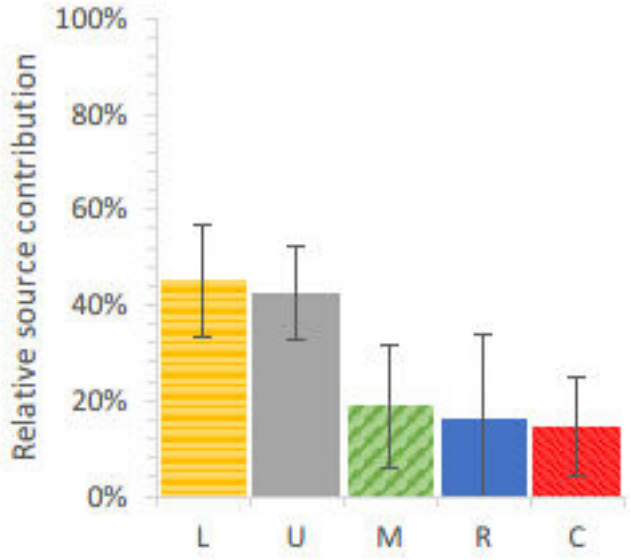

Figure 2: Average relative sediment source contributions (%) to the suspended sediment. Error bars represent the 95% confidence intervals. (Sediment sources: grassland from the limestone (L), Millstone grit (M), coals measures (C) areas, riverbanks (R), and urban street dust (U))

Variation in suspended sediment sources

(i) Inter-event variation

The varying relationship between SSC, discharge, and source contributions at the inter-event scale is illustrated in the time series of multiple discharge peaks in November 2016 and February 2017 (Figure 3). As discharge peaks in November 2016 progressed, limestone SSC (SSC_L) appeared to decrease, while coals SSC (SSC_C) slightly increased. Furthermore, urban street dust SSC (SSC_U) appeared to be highest during the rising limb of the hydrographs, remaining an important source throughout the events, while riverbank SSC ($SSC_{R)}$ was slightly higher during the second half of the discharge peaks, despite the uncertainty associated with SSC_R estimations (Figure 3 a). Similar trends in SSC_L and SSC_C were evident in discharge peaks in February

2017, while total SSC (SSC_t) appeared to decrease despite similar discharge peaks (Figure 3 b).

While events in November 2016 were generally characterised by highest discharges and SSCs, smaller events, in terms of discharge, were also observed with high SSCs that were linked to different sources (Table 2). For example, compared to other events, Jun-16 (1) was characterised by a low Q_{max} (31 m^3 s^{-1}) and P_{7d} (12 mm), but relatively high SSCs (107 mg L^{-1}) and a dominant contribution from urban street dust. Another example is the event Sep-16, which had an average Q_{max} (43.3 m^3 s^{-1}), but exceptionally high SSCs (1007.5 mg L^{-1}) with dominant contributions from eroding riverbanks.

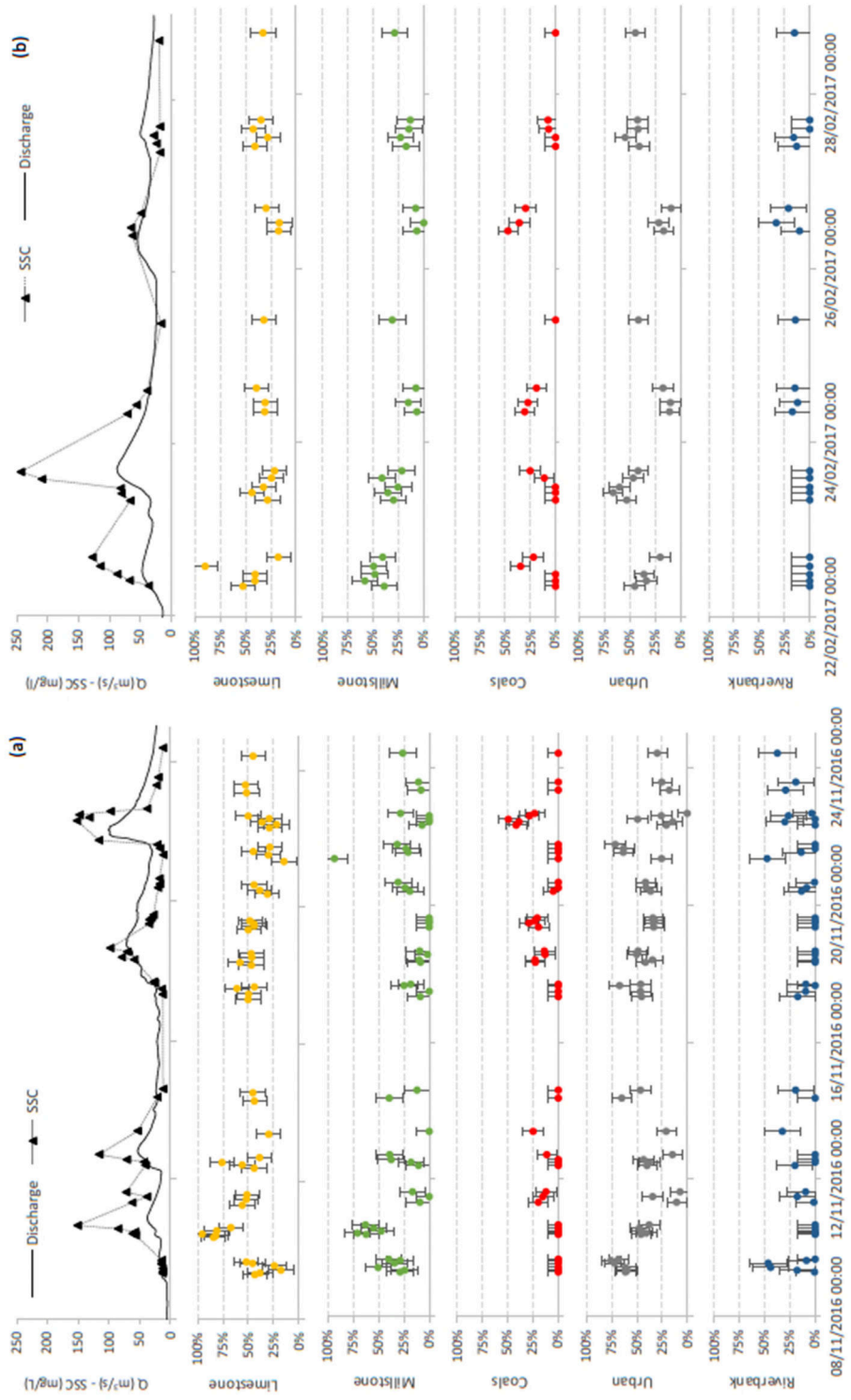

Figure 3: Discharge (Q) and sampled suspended sediment concentration (SSC) with estimated relative sediment source contributions (%) with associated confidence intervals (Table 1) for sampled events in: (a) November 2016 and (b) February 2017.

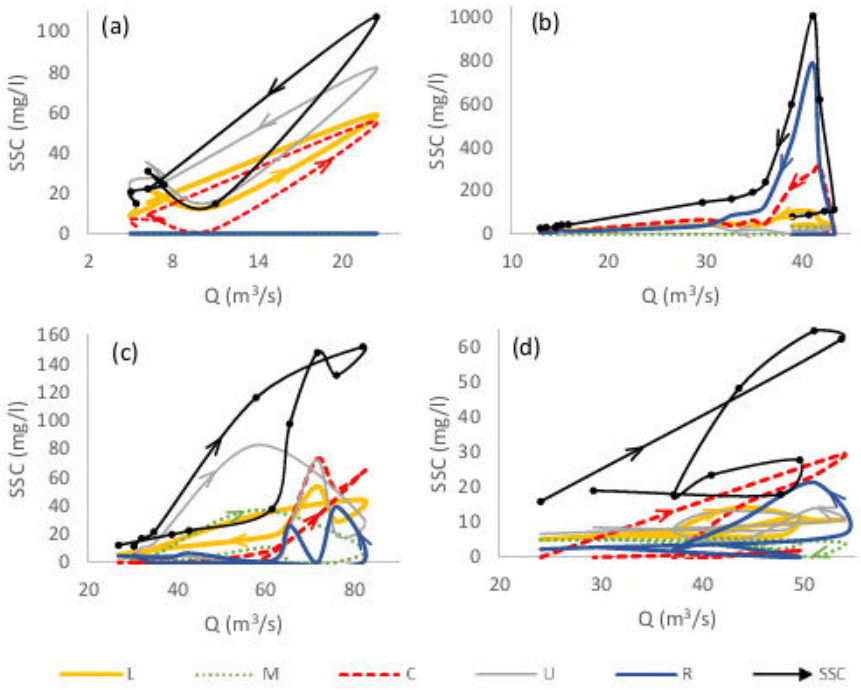

Figure 4: Hysteresis patterns between suspended sediment concentration (SSC) and discharge (Q) with estimated source-specific SSCs during high-flow events in (a) Jun-16(1), (b) Sep-16, (c) Nov-16(4), and (d) Feb-17(2) (Sediment sources: grassland from the limestone (L), Millstone grit (M), coals measures (C) areas, riverbanks (R), and urban street dust (U)). Note that confidence intervals associated with the source-specific SSCs as shown in Table 1 should be considered.

Table 2: Hydro-meteorological and sediment variables per event ($SSC_{mean,\ max\ ,\ min,\ L,\ M,\ C,\ U,\ R}$: suspended sediment concentration (mg L^{-1}) mean, maximum, minimum, mean limestone, millstone, coals, urban and riverbank; $Q_{mean,\ max}$: discharge ($m^3\ s^{-1}$) mean and maximum; $P_{1d,\ 7d,\ 21d}$: precipitation (mm) 1-7-21day antecedent totals).

	# SS samples	SSC_{mean}	SSC_{max}	SSC_{min}	SSC_L*	SSC_M*	SSC_C*	SSC_U*	SSC_R*	Q_{mean}	Q_{max}	P_{1d}	P_{7d}	P_{21d}
Aug-15	12	29.1	90.6	7.0	24.7	2.5	2.9	13.3	11.9	21.5	74.1	13.1	28.2	69.3
Nov-15	16	33.9	46.7	14.7	16.8	0.0	1.6	14.1	6.1	72.3	122.0	5.3	16.0	158.6
Mar-16	6	19.8	27.4	12.5	12.4	4.3	0.0	15.5	0.0	26.7	40.9	0.5	53.8	81.9
Jun-16(1)	10	28.2	107.3	8.7	21.1	0.0	13.5	31.8	0.0	9.4	31.1	7.2	11.9	44.2
Jun-16(2)	6	47.1	103.4	8.3	19.2	0.0	33.5	31.9	0.0	16.5	30.7	10.6	33.2	49.0
Aug-16	6	15.9	18.7	13.0	7.7	2.3	0.0	7.0	4.9	13.5	23.2	15.0	54.2	81.4
Sep-16	23	179.4	1007.5	7.4	39.4	7.3	66.0	15.1	115.8	18.8	43.3	14.2	20.1	64.8
Nov-16(1)	15	42.8	151.0	3.3	31.6	20.9	1.9	17.9	2.1	18.2	37.6	2.7	8.4	22.2
Nov-16(2)	8	51.7	116.0	11.7	24.4	13.4	3.8	15.7	3.9	28.4	53.4	0.3	27.4	34.0
Nov-16(3)	16	37.6	97.8	12.3	18.1	3.3	5.6	15.9	0.7	47.0	72.0	4.8	44.7	57.7
Nov-16(4)	13	65.6	152.0	11.2	20.9	7.0	18.7	22.5	7.4	48.4	101.0	3.1	47.3	88.7
Jan-17	6	12.0	21.6	3.7	5.3	3.6	0.0	3.7	4.8	18.5	29.5	0.6	15.8	37.8
Feb-17(1)	14	98.3	243.5	36	34.2	33.3	14.9	46.3	1.7	37.8	88.2	6.24	12.82	50.42
Feb-17(2)	8	33.0	64.8	15.9	8.6	3.8	7.1	9.4	5.1	34.4	54.5	6.62	35.64	61.36

*Note that confidence intervals associated with the source-specific SSCs as shown in Table 1 should be considered.

(ii) Intra-event variation

At the intra-event scale, discharge-SSC hysteresis patterns further illustrate the temporal variation in SS transport and sources (Figure 4). Most significantly, based on the samples taken, the source-specific SSCs do not always follow the same hysteresis pattern (i.e. the source contributions are not constant or equally important throughout events).

In Jun-16(1) a slight counter-clockwise pattern was observed, with urban street dust as the dominant SS source (Figure 4 a). Furthermore, the hysteresis patterns of SSC_t, SSC_L, SSC_C and SSC_U exhibited a consistent counter-clockwise pattern, while SSC_R and SSC_M were close to zero. Contrarily, the counter-clockwise hysteresis pattern in Sep-16 was characterised by slightly higher discharges and a very high SSC peak (Figure 4 b). At the start of the event, SSC_R, SSC_L, and SSC_C increased consistently with SSC, and riverbank became the dominant SS source. However, SSC_R decreased rapidly towards the end of the event, while SSC_C decreased more gradually, which coincided with a slight increase of SSC_U. Furthermore, the Nov-16(4) event exhibited a clockwise-pattern whereby the dominant sediment source changed from urban street dust during the rise of the hydrograph, to coals grassland at peak discharges, and limestone grassland during the falling limb (Figure 4 c). SSC_L, SSC_C, and SSC_U hysteresis patterns were consistent with total SSC, all showing a second SSC peak during the falling limb of the hydrograph, while in SSC_R a double peak was present before and after the second SSC peak. Finally, Feb-17(2) was characterised by a complex hysteresis pattern with a counter-clockwise loop during the first peak, and a smaller clockwise during the second peak (Figure 4 d). The first peak was mainly

characterised by SSC_C (clockwise) and SSC_R (counter-clockwise). During the second peak, SSC_L and SSC_U became dominant, both displaying a clockwise pattern.

Hydro-meteorological drivers

The temporal analyses illustrated that total SSCs, SS sources and hydro-meteorological variables vary substantially between and during high-flow events. In what follows, correlations and relationships between SSCs and hydro-meteorological variables are further investigated to identify potential drivers for the observed temporal patterns.

(i) Pairwise correlations

The Pearson Correlation analysis confirmed significant correlations between SSC and hydro-meteorological variables (Table 4). Correlations existed between total SSCs and source-specific SSCs: SSC_t was positively correlated with SSC_L, SSC_C, SSC_R, while negatively correlated with SSC_U. Most discharge variables were also significantly correlated with precipitation variables, and strong correlations existed between precipitation variables at different monitoring stations.

Furthermore, SSCs were correlated to various hydro-meteorological variables (Table 4). SSC_t was correlated to discharge, P_{1d} and P_{7d} (mainly from PH). SSC_L and SSC_u were positively correlated with instantaneous precipitation, while negatively correlated with discharge and antecedent precipitation. A similar correlation was present for SSC_C, mostly with precipitation variables at MT. Contrarily, SSC_M was positively correlated with antecedent discharge (Q_{21d}) and SSC_R was positively correlated to antecedent precipitation at PH.

(ii) Predictive relationships

The results of the Pearson Correlation analysis demonstrated covariation between many hydro-meteorological variables, which emphasizes the need to use statistical techniques such as PLSR which can handle high degrees of variable covariation. PLSR models were developed to estimate total and source-specific SSCs as a function of hydro-meteorological variables (Table 3, supplementary material). The SSC_L-PLSR model had the highest goodness of fit (R^2 = 56.2%), while the root mean squared error of prediction (RMSEP) was highest for SSC_t-PLSR (56.6 mg L^{-1}), which is partly attributed to the exceptionally high total SSCs during the event in September 2016. Generally, the models consisted of 4 to 6 components with a varying explained variance between 42% and 57%. In all models, the first component explained significantly more variance than the second component.

Table 3: Model statistics of Partial Least Squares regression between SSCs (Y) (total and source-specific) and hydro-meteorological variables (X) (RMSEP: root mean squared error of prediction).

	SSC_t	SSC_L*	SSC_M*	SSC_C*	SSC_U*	SSC_R*
R^2 (%)	36.4	56.2	29.7	48.5	28.7	32.3
RMSEP (mg L^{-1})	56.6	10.7	10.4	27	12.8	42.8
Number of components	5	5	6	4	4	5
Explained variance 1st component (%)	32.57	41.51	26.98	20.99	33.09	15.13
Explained variance 2nd component (%)	5.07	6.33	8.95	8.69	2.91	3.92
Explained variance all components (%)	56.2	57.53	41.88	48.51	49.93	31.08

*Note that confidence intervals associated with the source-specific SSCs as shown in Table 1 were not taken into account in this analysis.

The loadings associated to the PLSR models were further examined to identify which hydro-meteorological variables define the model components (Figure 5). The SSC_t and SSC_L models were defined by a similar set of variables, with the first component

determined by P_{1d} and Q (instantaneous precipitation and discharge), and the second component by P_{7d}, $P_{21}d$, Q_{1d} and Q_{7d} (antecedent precipitation and discharge).

The other source-specific SSCs appeared to be best predicted by a different combination of variables, suggesting the presence of different driving factors. In general, in the SSC_M, SSC_C, and SSC_U models, precipitation variables at MT and TR were most important. Furthermore, both the SSC_M and SSC_C models were defined by the inverse of the SSC_L model, with the first component determined by P_{7d} and P_{21d} and Q_{7d} (antecedent precipitation and discharge), and the second component by Q and P_{1d} (instantaneous precipitation and discharge). The SSC_U model was determined by P_{1d} in the first component, and Q in the second component (both instantaneous). Contrarily, the SSC_R model was mainly determined by precipitation at PH (first component), while a wide range of variables defined the second component.

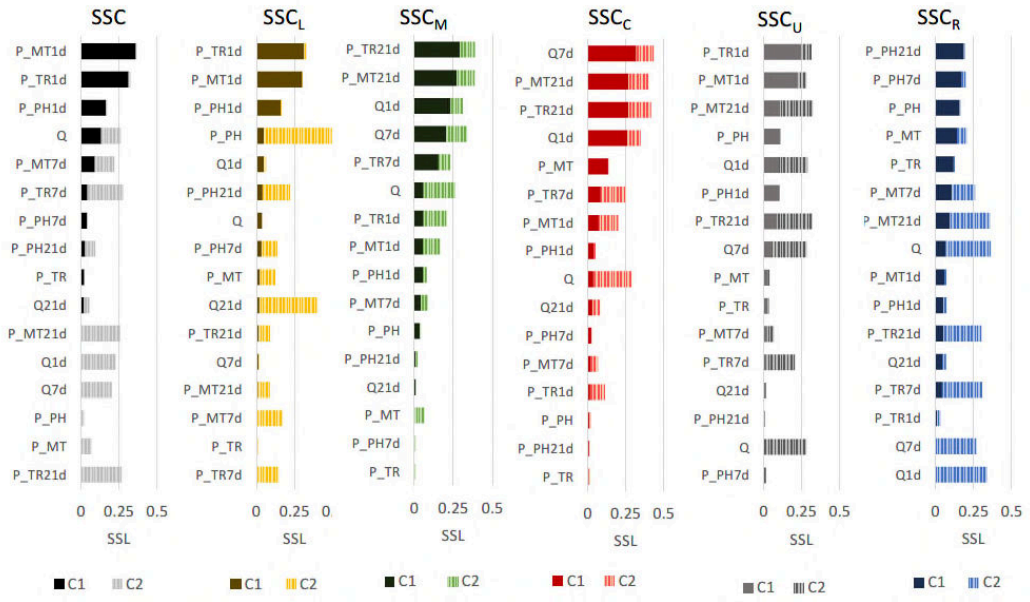

Figure 5: Sum of squared loadings (SSL) of the first two components (C1 and C2) of the SSC-PLSR models. Sediment sources: grassland from the limestone (L), Millstone grit (M), coals measures (C) areas, riverbanks (R), and urban street dust (U). Note that confidence intervals associated with the source-specific SSCs as shown in Table 1 were not taken into account in this analysis.

Table 4: Pearson correlation analysis between SSC, Source-specific SSCs and hydro-meteorological variables (Q: discharge, P: precipitation, 1, 7 and 21 days antecedent Q and P). Bold numbers are significant at the 95% confidence level.

	SSC	SSC_L*	SSC_M*	SSC_C*	SSC_U*	SSC_R*	Q	Q_{1d}	Q_{7d}	Q_{21d}	P_{TR}	P_{TR1d}	P_{TR7d}	P_{TR21d}	P_{PH}	P_{PH1d}	P_{PH7d}	P_{PH21d}	P_{MT}	P_{MT1d}	P_{MT7d}	P_{MT21d}
SSC	1.00																					
SSC_L	**-0.36**	1.00																				
SSC_M	-0.08	0.10	1.00																			
SSC_C	**0.24**	-0.16	**-0.46**	1.00																		
SSC_U	**-0.32**	**0.52**	0.06	0.07	1.00																	
SSC_R	**0.41**	**-0.52**	**-0.22**	0.00	**-0.51**	1.00																
Q	**0.19**	**-0.23**	-0.10	-0.07	**-0.30**	-0.09	1.00															
Q_{1d}	**-0.20**	-0.05	**-0.22**	**-0.21**	**-0.21**	-0.02	**0.59**	1.00														
Q_{7d}	-0.11	0.06	-0.16	**-0.21**	0.00	0.00	**0.62**	**0.73**	1.00													
Q_{21d}	0.07	0.07	**0.24**	**-0.25**	0.09	0.01	-0.16	-0.02	0.06	1.00												
P_{TR}	-0.06	0.16	-0.05	0.00	**0.27**	-0.12	-0.09	0.01	0.07	0.01	1.00											
P_{TR1d}	**0.30**	0.12	**0.19**	0.04	0.05	**-0.23**	**0.51**	0.02	**0.19**	-0.04	0.06	1.00										
P_{TR7d}	-0.10	-0.04	**-0.34**	0.08	-0.07	-0.08	**0.64**	**0.68**	**0.58**	-0.15	-0.01	**0.27**	1.00									
P_{TR21d}	-0.09	0.08	**-0.31**	-0.14	-0.06	0.11	**0.56**	**0.68**	**0.84**	-0.05	0.00	0.16	**0.76**	1.00								
P_{PH}	-0.09	**0.21**	0.03	0.00	**0.29**	**-0.20**	-0.09	-0.02	0.09	-0.01	**0.20**	0.15	0.03	0.00	1.00							
P_{PH1d}	**0.60**	-0.13	0.05	0.10	**-0.23**	**0.21**	0.12	**-0.33**	-0.16	0.08	-0.06	**0.52**	-0.04	-0.04	0.00	1.00						
P_{PH7d}	**0.25**	-0.07	**-0.28**	0.11	**-0.33**	**0.31**	-0.14	**-0.23**	**-0.34**	**-0.19**	-0.11	0.09	0.10	0.00	-0.08	0.46	1.00					
P_{PH21d}	0.14	-0.02	-0.11	-0.16	**-0.42**	**0.28**	0.11	0.04	0.01	**-0.19**	-0.10	0.08	0.17	**0.23**	0.06	**0.32**	0.73	1.00				
P_{MT}	-0.10	**0.24**	0.08	-0.15	**0.18**	**-0.22**	0.14	**0.27**	**0.39**	0.07	**0.21**	**0.20**	**0.20**	**0.26**	**0.57**	-0.05	**-0.19**	0.08	1.00			
P_{MT1d}	**0.45**	-0.12	0.13	**0.18**	-0.14	-0.11	**0.51**	-0.15	0.00	**-0.21**	-0.05	**0.74**	**0.20**	0.06	0.04	**0.66**	0.12	0.11	0.03	1.00		
P_{MT7d}	-0.04	**-0.25**	-0.03	**-0.32**	**-0.42**	0.04	**0.60**	**0.45**	**0.22**	**-0.18**	-0.14	0.06	**0.52**	**0.29**	-0.05	-0.03	**0.19**	**0.41**	0.09	**0.19**	1.00	
P_{MT21d}	0.00	-0.07	**-0.22**	**-0.29**	**-0.28**	**0.22**	**0.64**	**0.66**	**0.81**	-0.05	-0.06	0.10	**0.63**	**0.91**	-0.05	0.03	0.06	**0.38**	**0.23**	0.11	**0.52**	1.00

*Note that confidence intervals associated with the source-specific SSCs as shown in Table 1 were not taken into account in this analysis.

Discussion

This study combined high frequency monitoring of SSC during high-flow events with DRIFTS-based sediment fingerprinting to investigate the influence of SS source contributions and hydro-meteorological variables on temporal variations in SSC. Considerable temporal variability in SSCs and sources was observed during the monitored high-flow events, which can be linked to different hydro-meteorological variables and sediment transport process interactions.

Total suspended sediment concentration

Total SSC in the River Aire varied considerably during and between different rainfall events. High-flow events of similar discharge exhibited differing peak SSCs and strong intra-event variation (Figure 3). Significant correlation was found between total SSC and instantaneous precipitation and discharge (Table 3), which was also expressed in the PLSR components (Figure 5), suggesting the presence of a fast-response SS transport system (Bracken et al., 2015). Nevertheless, the predictive power of the PLSR model to estimate SSCs based on the chosen hydro-meteorological variables was generally low (R^2 of 36.4%), which indicates the difficulty in capturing variations in SSCs over time and could partially be explained by source-specific process interactions controlling total SSCs.

Suspended sediment sources and drivers

This study is one of the first of its kind to combine sediment fingerprinting at the event-scale with an analysis of the temporal variation in SSCs and hydro-meteorological variables in order to identify source-specific factors and process interactions controlling total SSC. This type of analysis is made possible thanks to the recent

development of a time-and cost efficient sediment fingerprinting approach (Poulenard et al., 2012), and the availability of detailed hydro-metereolofical data within the catchment. However, the predictive power of the PLSR models to estimate source-specific SSCs is generally low, with the models for SSC_L and SSC_C performing better compared to SSC_t, while the other sources perform equally poor (Table 4). Therefore, any interpretation of the results needs to be done with consideration of these uncertainties. A more in-depth discussion on methodological considerations for future research is presented in the next section.

(i) Sediment from urban areas

High contributions from urban street dust were observed, reflecting the urban location of the point of sampling, which is in agreement with other studies within the Aire catchment that observed a significant impact from the urban environment on SSCs (Carter et al., 2003; Old et al., 2006) and SS-associated contaminants (Walling et al., 2003a).

Furthermore, the average street dust contribution during individual events was most strongly correlated to instantaneous discharge and precipitation (Figure 5). These results suggest that street dust contribution responds fast to precipitation and varies relatively constant with the total SSC (Figure 3, 4), which demonstrates the proximity of urban area to the sampling location and the high degree of connectivity of the urban area to the river system (i.e. stormwater drainage system) (Figure 6).

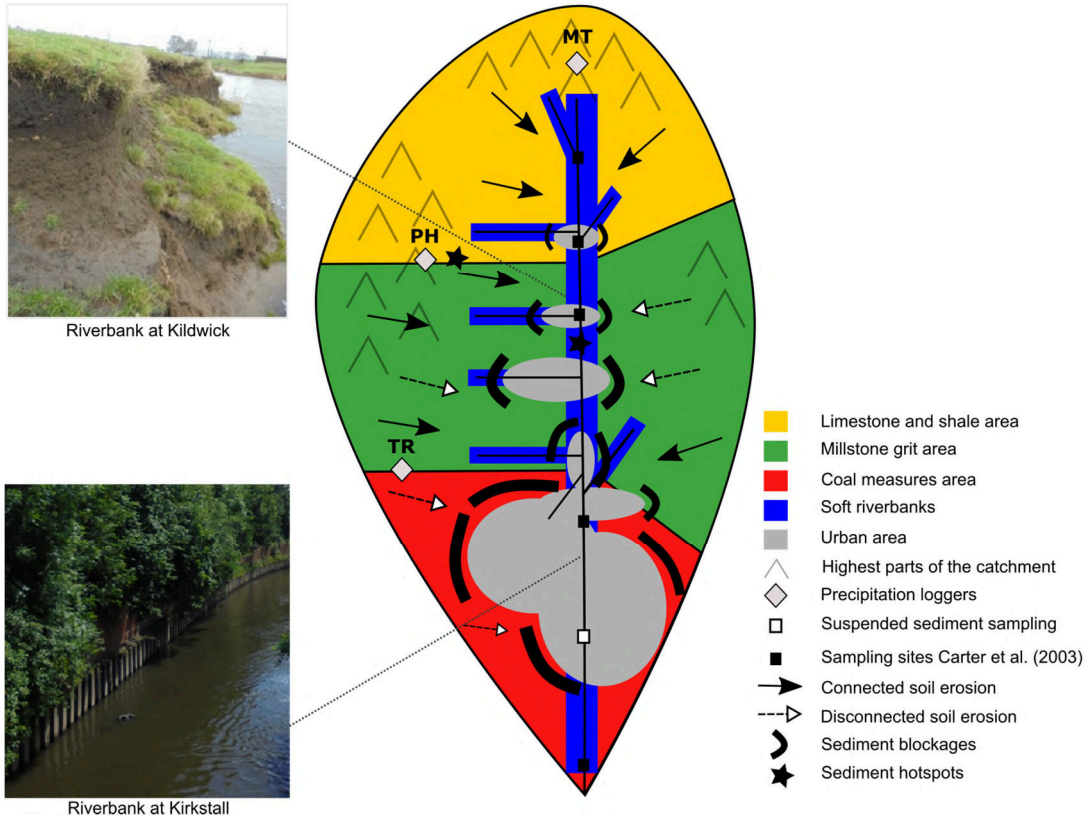

Figure 6: Conceptual illustration of the suspended sediment transport dynamics and connectivity in the River Aire catchment.

(ii) Sediment from grassland areas

Even though grassland is generally considered to be less prone to soil erosion compared to arable land (i.e. presence of protective vegetation cover), considerable contributions of sediment from grassland areas to the SS were found in the River Aire. These high contributions could be the result of cattle grazing in the catchment (i.e. trampling causing detachment and mobilisation of sediment particles or causing flow paths) (Bilotta et al., 2007; James and Alexander, 1998; Meyles et al., 2006; Peukert et al., 2014; Trimble and Mendel, 1995). Nevertheless, not all grassland areas were equally important in contributing to the SS, which appears to be controlled by the

combination of antecedent precipitation and sediment connectivity (i.e. the capacity of the catchment to effectively transfer material towards the river determined by the presence/absence of physical blockages such as hills, ditches or plains) (Fryirs, 2013). In this study, urban areas are considered as main blockages preventing sediment from grassland areas to be transferred to the river system by obstructing (natural) flow paths as a result of e.g. build-up areas, parks and gardens, ditches and road verges (Figure 6).

Sediment from limestone grassland (SSC_L) was most strongly correlated to total SSC and showed a similar correlation to event-based hydro-meteorological variables (P_{1d} and Q). This corresponds with the observation that limestone grassland was the dominant sediment source in the River Aire during the monitored period (Figure 2) and that limestone grassland contribution remained significant throughout events (e.g. Figure 4). However, the limestone area is also the most distant source area from the point of sampling (40 to 45 km). These findings could indicate that a ready-available supply of limestone grassland sediment is available within the river system (e.g. stored on the river bed) (Poulenard et al., 2012; Sherriff et al., 2016). The presence of a high limestone-sediment supply could possibly be explained by higher erosion rates in the upper part of the catchment due to the steeper topography and higher connectivity of the landscape to the river (i.e. predominantly grassland with few urbanised areas) compared to the other grassland areas (Fryirs, 2013) (Figure 6). This hypothesis is supported by the observation that precipitation from PH (located in a steep part of the catchment; Figure 1) was especially correlated to the SSC_L.

Contrarily, SSCs from the millstone and coals grassland were mainly correlated to antecedent precipitation and discharge. The middle and lower parts of the catchment are characterised by more gentle slopes, and the grassland areas are often not directly connected to the river system due to a higher degree of urbanisation (Figure 1 and 6). Especially the coals grassland area is very scattered within predominant urban area and is not well connected to the river system. This hypothesis would imply that more prolonged precipitation (i.e. antecedent precipitation) is required to connect (or transfer) the eroded material to the river system (Fryirs, 2013), and could also explain the lag-time in the coals grassland contribution during events (Figure 3 and 4).

(iii) Sediment from eroding riverbanks

Riverbank material was not found to be a dominant source of SSC at the point of sampling and was the least well correlated to hydro-meteorological factors. Part of this lack of correlation is likely linked to the low degree of discrimination of riverbank material form other source material and the associated high uncertainty on the estimated contributions.

Nevertheless, the lack of correlation with hydro-meteorological variables could also be explained by the episodic, less predictable, nature of riverbank erosion such as riverbank collapse, which would result in a sudden contribution as observed for the event in Sep-16 (Figure 4 b). Yet, the sampling frequency might not have been sufficient to have captured other sudden collapses of highly localized river banks. Furthermore, despite the high uncertainty, slight increases in riverbank contributions appear to be present towards the second-half of events (i.e. lag-time between the start of the event and increase in riverbank contribution) (Figure 3). This finding is

consistent with previous studies suggesting that most bank material is entrained at higher discharges (Janes et al., 2017; Rügner et al., 2014; Sear et al., 2003; Zeiger and Hubbart, 2016). In the upper part of the catchment (especially near Kildwick), riverbanks are strongly incised and visibly eroding (Figure 6), which could explain the correlation of riverbank sources to precipitation at PH. These observations are in agreement with findings from Carter et al. (2003), who observed a high relative contribution of riverbank in the upper part of the catchment. Contrarily, in the more urbanised parts of the catchment close to the point of sampling, riverbanks are protected by concrete embankments (Figure 6), which could present an alternative/additional explanation for the lag time in the riverbank contribution during events (i.e. eroding riverbanks are more distant to the point of sampling).

Methodological considerations

As discussed in the methodology, the sediment fingerprinting method used in this study presents tremendous opportunities to investigate variations in SS sources at a fine temporal resolution because it is more time and cost efficient than traditional sediment fingerprinting methods (Poulenard et al., 2009). However, there are some methodological considerations to consider when interpreting the results.

First, the design of the sediment fingerprinting method used in this study (i.e. individual, source-specific PLSR models using DRIFTS) strongly differs from traditional sediment fingerprinting methods (i.e. based on a mass balance equation using geochemistry or fallout radionuclides) (Pulley and Collins, 2018). Because of these differences in design, standard techniques to assess the impact of particle size variations, source groupings, and tracer conservatism (Laceby et al., 2017) are not

directly transferable to the DRIFTS-PLSR method. Due to the experimental and explorative design of the study, these aspects, as well as error propagation across different analyses, were not investigated further but remain important steps to produce reliable results (Vercruysse and Grabowski, 2018). Towards future development and use of sediment fingerprinting to investigate sediment transport processes, further methodological testing with regards to particle size and conservatism will be required (Vercruysse and Grabowski, 2018), as well as exploring possibilities of combining different sediment fingerprinting methods. Especially in the case for riverbank material, combination with other methods is advisable, by for example using DRIFTS with X-ray fluorescence spectroscopy and geochemistry (Cooper et al., 2014b, 2014a).

Furthermore, comparison of results in this study with a previous sediment fingerprinting study in the Aire catchment (Carter et al., 2003), indicates two other critical methodological aspects that need to be considered. First, Carter et al. (2003) used submersible pumps to collect 70 SS samples between November 1997 and January 1999 (mostly) during high-flow events. Contrarily, this study is based on a more extensive dataset of 159 SS samples taken during 14 high-flow events between June 2015 and March 2017 with a depth-integrating sampler. While still based on discrete manual samples, the sampling design of this study allowed the investigation of variations in SS sources at a much finer temporal resolution, which enabled the identification of significant variation depending on the time of sampling. Second, while in this study all SS samples were taken at a single location within Leeds city centre (reflected in the high urban contribution to SS), Carter et al. (2003) took SS samples at five locations upstream of the city centre (Figure 6). Due to their spatially distributed

study design, it was demonstrated that dominant SS sources vary considerable along the profile of the river.

In short, interpretation of SS source information in terms of drivers for SS transport will be influenced by the timing, frequency, and location of SS sampling. To capture the full spatiotemporal variation in SS transport, it is essential to take SS samples during different high-flow events throughout the year and in succession, while also adopting a spatially distributed sampling campaign (Perks et al., 2017).

Conclusion

This study demonstrated the potential and importance of combining sediment fingerprinting with statistical analysis of hydro-meteorological data to investigate temporal variation in SSCs in rivers in terms of varying source contributions and hydro-meteorological variables and to gain better understanding of sediment connectivity at the catchment scale.

In general, contributions from street dust and limestone grassland follow similar patterns as the total SSC at the sampled location in the River Aire, indicating the location and erosion dynamics of these source areas (i.e. fast mobilisation to and within river). Contrarily, contributions from millstone and coals grassland are less consistent, and driven by antecedent hydro-meteorological conditions (i.e. lag-time between soil erosion and sediment delivery to river). Riverbank material was poorly correlated to hydro-meteorological factors. While this lack of correlation is likely linked to the low degree of discrimination of riverbank material form other source material, it could also be linked to the more episodic nature of riverbank erosion (i.e. bank collapse).

These differences in source-specific drivers and processes for sediment transport demonstrate the difficulty in generalising sediment transport patterns. The presented methodology and associated interpretation of results creates opportunities towards evaluating temporal variation in SSCs from a catchment perspective. Further advancement of the approach, including identification of different sources of uncertainty associated with the DRIFTS-based method and subsequent multivariate analysis, will help the development of source-specific erosion and sediment transport models and inform targeted soil and water conservation plans, both in terms of quantity (i.e. when is SSC too high) and quality (i.e. where does SS come from).

Acknowledgments

This research was funded by an industrial PhD studentship supported by Cranfield University, Leeds City Council and Ove Arup and Partners Limited. The authors would like to specifically thank Tim Hess (Cranfield University) for editorial support, and Irantzu Lexartza-Artza, Milly Hennayake, and Sally German (Arup) for helping to organise the fieldwork. Suspended sediment concentrations and raw DRIFTS spectra of sediment and soil samples can be downloaded from the Cranfield Online Research Data portal (DOI: 10.17862/cranfield.rd.5903923).

References

Aich V, Zimmermann A, Elsenbeer H. 2014. Quantification and interpretation of suspended-sediment discharge hysteresis patterns: How much data do we need? Catena **122** : 120–129. DOI: 10.1016/j.catena.2014.06.020 [online] Available from: http://dx.doi.org/10.1016/j.catena.2014.06.020

Alexandrov Y, Laronne JB, Reid I. 2007. Intra-event and inter-seasonal behaviour of suspended sediment in flash floods of the semi-arid northern Negev, Israel. Geomorphology **85** : 85–97. DOI: 10.1016/j.geomorph.2006.03.013

Belmont P et al. 2011. Large shift in source of fine sediment in the upper Mississippi

River. Environmental Science and Technology **45** : 8804–8810. DOI: 10.1021/es2019109

Bilotta GS, Brazier RE. 2008. Understanding the influence of suspended solids on water quality and aquatic biota. Water Research **42** : 2849–2861. DOI: 10.1016/j.watres.2008.03.018

Bilotta GS, Brazier RE, Haygarth PM. 2007. The Impacts of Grazing Animals on the Quality of Soils, Vegetation, and Surface Waters in Intensively Managed Grasslands. Advances in Agronomy **94** : 237–280. DOI: 10.1016/S0065-2113(06)94006-1

Bilotta GS, Burnside NG, Cheek L, Dunbar MJ, Grove MK, Harrison C, Joyce C, Peacock C, Davy-Bowker J. 2012. Developing environment-specific water quality guidelines for suspended particulate matter. Water Research **46** : 2324–2332. DOI: 10.1016/j.watres.2012.01.055 [online] Available from: http://dx.doi.org/10.1016/j.watres.2012.01.055

Bracken LJ, Turnbull L, Wainwright J, Bogaart P. 2015. Sediment connectivity: a framework for understanding sediment transfer at multiple scales. Earth Surface Processes and Landforms **40** : 177–188. DOI: 10.1002/esp.3635 [online] Available from: http://doi.wiley.com/10.1002/esp.3635

British Geological Survey. 2016. The BGS Lexicon of Named Rock Units. : Last viewed on 25/10/16. [online] Available from: http://www.bgs.ac.uk/lexicon/home.html

Carter J, Owens PN, Walling DE, Leeks GJL. 2003. Fingerprinting suspended sediment sources in a large urban river system. The Science of The Total Environment **314–316** : 513–534. DOI: 10.1016/S0048-9697(03)00071-8 [online] Available from: http://linkinghub.elsevier.com/retrieve/pii/S0048969703000718 (Accessed 16 October 2014)

Carter J, Walling DE, Owens PN, Leeks GJL. 2006. Spatial and temporal variability in the concentration and speciation of metals in suspended sediment transported by the River Aire, Yorkshire, UK. Hydrological Processes **20** : 3007–3027. DOI: 10.1002/hyp.6156 [online] Available from: http://doi.wiley.com/10.1002/hyp.6156 (Accessed 3 November 2014)

Chen F, Zhang F, Fang N, Shi Z. 2016. Sediment source analysis using the fingerprinting method in a small catchment of the Loess Plateau, China. Journal of Soils and Sediments DOI: 10.1007/s11368-015-1336-7 [online] Available from: http://link.springer.com/10.1007/s11368-015-1336-7

Collins AL, Foster IDL, Gellis AC, Porto P, Horowitz AJ. 2017. Sediment source fingerprinting for informing catchment management: Methodological approaches, problems and uncertainty. Journal of Environmental Management **194** : 1–3. DOI: 10.1016/j.jenvman.2017.03.026 [online] Available from: http://dx.doi.org/10.1016/j.jenvman.2017.03.026

Cooper RJ, Krueger T, Hiscock KM, Rawlins BG. 2014a. High-temporal resolution fluvial sediment source fingerprinting with uncertainty: A Bayesian approach. Earth

Surface Processes and Landforms DOI: 10.1002/esp.3621 [online] Available from: http://doi.wiley.com/10.1002/esp.3621 (Accessed 27 October 2014)

Cooper RJ, Rawlins BG, Lézé B, Krueger T, Hiscock KM. 2014b. Combining two filter paper-based analytical methods to monitor temporal variations in the geochemical properties of fluvial suspended particulate matter. Hydrological Processes **28** : 4042–4056. DOI: 10.1002/hyp.9945 [online] Available from: http://doi.wiley.com/10.1002/hyp.9945 (Accessed 20 October 2014)

Davis CM, Fox JF. 2009. Sediment Fingerprinting : review of the method and future improvements for allocating nonpoint source pollution. Journal of environmental engineering **137** : 490–505.

Eder A, Strauss P, Krueger T, Quinton JN. 2010. Comparative calculation of suspended sediment loads with respect to hysteresis effects (in the Petzenkirchen catchment, Austria). Journal of Hydrology **389** : 168–176. DOI: 10.1016/j.jhydrol.2010.05.043 [online] Available from: http://dx.doi.org/10.1016/j.jhydrol.2010.05.043

Fan X, Shi C, Zhou Y, Shao W. 2012. Sediment rating curves in the Ningxia-Inner Mongolia reaches of the upper Yellow River and their implications. Quaternary International **282** : 152–162. DOI: 10.1016/j.quaint.2012.04.044 [online] Available from: http://dx.doi.org/10.1016/j.quaint.2012.04.044

Fang NF, Shi ZH, Chen FX, Zhang HY, Wang YX. 2015. Discharge and suspended sediment patterns in a small mountainous watershed with widely distributed rock fragments. Journal of Hydrology **528** : 238–248. DOI: 10.1016/j.jhydrol.2015.06.046 [online] Available from: http://linkinghub.elsevier.com/retrieve/pii/S002216941500459X

Francke T, Lopez-Tarazon JA, Vericat D, Bronstert A, Batalla RJ. 2008. Flood-based analysis of high-magnitude sediment transport using a non-parametric method. Earth Surface Processes and Landforms **33** : 2064–2077. DOI: 10.1002/esp. 1654 [online] Available from: http://www3.interscience.wiley.com/journal/121517813/abstract

Francke T, Werb S, Sommerer E, López-Tarazón JA. 2014. Analysis of runoff, sediment dynamics and sediment yield of subcatchments in the highly erodible Isábena catchment, Central Pyrenees. Journal of Soils and Sediments **14** : 1909–1920. DOI: 10.1007/s11368-014-0990-5 [online] Available from: http://link.springer.com/10.1007/s11368-014-0990-5 (Accessed 17 November 2014)

Franz C, Makeschin F, Weiß H, Lorz C. 2014. Sediments in urban river basins: identification of sediment sources within the Lago Paranoá catchment, Brasilia DF, Brazil - using the fingerprint approach. The Science of the total environment **466**–**467** : 513–23. DOI: 10.1016/j.scitotenv.2013.07.056 [online] Available from: http://www.ncbi.nlm.nih.gov/pubmed/23933453 (Accessed 28 October 2014)

Fryirs KA. 2013. (Dis)Connectivity in catchment sediment cascades: A fresh look at the sediment delivery problem. Earth Surface Processes and Landforms **38** : 30–46. DOI: 10.1002/esp.3242

Gao P, Nearing M a., Commons M. 2013. Suspended sediment transport at the instantaneous and event time scales in semiarid watersheds of southeastern Arizona, USA. Water Resources Research **49** : 6857–6870. DOI: 10.1002/wrcr.20549

De Girolamo AM, Pappagallo G, Lo Porto A. 2015. Temporal variability of suspended sediment transport and rating curves in a Mediterranean river basin: The Celone (SE Italy). Catena **128** : 135–143. DOI: 10.1016/j.catena.2014.09.020 [online] Available from: http://linkinghub.elsevier.com/retrieve/pii/S0341816215000090

Grabowski RC, Gurnell AM. 2016. Diagnosing problems of fine sediment delivery and transfer in a lowland catchment. Aquatic Sciences **78** : 95–106. DOI: 10.1007/s00027-015-0426-3

James PA, Alexander RW. 1998. Soil erosion and runoff in improved pastures of the Clwydian Range, North Wales. Journal of Agricultural Science **130** : 473–488. DOI: 10.1017/S0021859698005425

Janes V, Nicholas A, Collins A, Quine T. 2017. Analysis of fundamental physical factors influencing channel bank erosion: results for contrasting catchments in England and Wales. Environmental Earth Sciences **76** DOI: 10.1007/s12665-017-6593-x

Karaman I, Qannari EM, Martens H, Hedemann MS, Knudsen KEB, Kohler A. 2013. Comparison of Sparse and Jack-knife partial least squares regression methods for variable selection. Chemometrics and Intelligent Laboratory Systems **122** : 65–77. DOI: 10.1016/j.chemolab.2012.12.005

Laceby JP, Evrard O, Smith HG, Blake WH, Olley JM, Minella JPG, Owens PN. 2017. The challenges and opportunities of addressing particle size effects in sediment source fingerprinting: A review. Earth-Science Reviews **169** : 85–103. DOI: 10.1016/j.earscirev.2017.04.009 [online] Available from: http://linkinghub.elsevier.com/retrieve/pii/S0012825216304548

Legout C, Poulenard J, Nemery J, Navratil O, Grangeon T, Evrard O, Esteves M. 2013. Quantifying suspended sediment sources during runoff events in headwater catchments using spectrocolorimetry. Journal of Soils and Sediments **13** : 1478–1492. DOI: 10.1007/s11368-013-0728-9 [online] Available from: http://link.springer.com/10.1007/s11368-013-0728-9 (Accessed 20 October 2014)

Lexartza-Artza I, Wainwright J. 2011. Making connections: Changing sediment sources and sinks in an upland catchment. Earth Surface Processes and Landforms **36** : 1090–1104. DOI: 10.1002/esp.2134

Lloyd CEM, Freer JE, Johnes PJ, Collins AL. 2016. Using hysteresis analysis of high-resolution water quality monitoring data, including uncertainty, to infer controls on nutrient and sediment transfer in catchments. Science of The Total Environment **543** : 388–404. DOI: 10.1016/j.scitotenv.2015.11.028 [online] Available from: http://linkinghub.elsevier.com/retrieve/pii/S0048969715310093

Martens H, Martens M. 2000. Modified Jack-knife estimation of parameter uncertainty

in bilinear modelling by partial least squares regression (PLSR). Food Quality and Preference **11** : 5–16. DOI: 10.1016/S0950-3293(99)00039-7

Martínez-Carreras N, Udelhoven T, Krein A, Gallart F, Iffly JF, Ziebel J, Hoffmann L, Pfister L, Walling DE. 2010. The use of sediment colour measured by diffuse reflectance spectrometry to determine sediment sources: Application to the Attert River catchment (Luxembourg). Journal of Hydrology **382** : 49–63. DOI: 10.1016/j.jhydrol.2009.12.017 [online] Available from: http://linkinghub.elsevier.com/retrieve/pii/S0022169409007951 (Accessed 5 November 2014)

Mauad CR, Wagener ADLR, Massone CG, Aniceto MDS, Lazzari L, Carreira RS, Farias CDO. 2015. Urban rivers as conveyors of hydrocarbons to sediments of estuarine areas: Source characterization, flow rates and mass accumulation. Science of The Total Environment **506**–**507** : 656–666. DOI: 10.1016/j.scitotenv.2014.11.033 [online] Available from: http://linkinghub.elsevier.com/retrieve/pii/S0048969714016155

Meyles EW, Williams AG, Ternan JL, Anderson JM, Dowd JF. 2006. The influence of grazing on vegetation, soil properties and stream discharge in a small Dartmoor catchment, southwest England, UK. Earth Surface Processes and Landforms **31** : 622–631. DOI: 10.1002/esp.1352 [online] Available from: http://www3.interscience.wiley.com/journal/121517813/abstract

Mukundan R, Walling DE, Gellis AC, Slattery MC, Radcliffe DE. 2012. Sediment source fingerprinting: transforming from a research tool to a management tool. Journal of the American Water Resources Association **48** : 1241–1257. DOI: 10.1111/j.1752-1688.2012.00685.x [online] Available from: http://doi.wiley.com/10.1111/j.1752-1688.2012.00685.x

Old GH, Leeks GJL, Packman JC, Smith BPG, Lewis S, Hewitt EJ. 2006. River flow and associated transport of sediments and solutes through a highly urbanised catchment, Bradford, West Yorkshire. Science of the Total Environment **360** : 98–108. DOI: 10.1016/j.scitotenv.2005.08.028

Onderka M, Krein A, Wrede S, Martínez-Carreras N, Hoffmann L. 2012. Dynamics of storm-driven suspended sediments in a headwater catchment described by multivariable modeling. Journal of Soils and Sediments **12** : 620–635. DOI: 10.1007/s11368-012-0480-6 [online] Available from: http://link.springer.com/10.1007/s11368-012-0480-6 (Accessed 4 November 2014)

Owens PN et al. 2005. Fine-grained sediment in river systems: environmental significance and management issues. River Research and Applications **21** : 693–717. DOI: 10.1002/rra.878 [online] Available from: http://doi.wiley.com/10.1002/rra.878

Owens PN, Blake WH, Gaspar L, Gateuille D, Koiter AJ, Lobb DA, Petticrew EL, Reiffarth DG, Smith HG, Woodward JC. 2016. Fingerprinting and tracing the sources of soils and sediments: Earth and ocean science, geoarchaeological, forensic, and human health applications. Earth-Science Reviews **162** : 1–23. DOI: 10.1016/j.earscirev.2016.08.012 [online] Available from:

http://dx.doi.org/10.1016/j.earscirev.2016.08.012

Palazón L, Latorre B, Gaspar L, Blake WH, Smith HG, Navas A. 2015. Comparing catchment sediment fingerprinting procedures using an auto-evaluation approach with virtual sample mixtures. Science of The Total Environment **532** : 456–466. DOI: 10.1016/j.scitotenv.2015.05.003 [online] Available from: http://www.sciencedirect.com/science/article/pii/S0048969715300619

Perks MT, Owen GJ, Benskin CMH, Jonczyk J, Deasy C, Burke S, Reaney SM, Haygarth PM. 2015. Dominant mechanisms for the delivery of fine sediment and phosphorus to fluvial networks draining grassland dominated headwater catchments. Science of The Total Environment **523** : 178–190. DOI: 10.1016/j.scitotenv.2015.03.008 [online] Available from: http://linkinghub.elsevier.com/retrieve/pii/S0048969715002739

Perks MT, Warburton J, Bracken LJ, Reaney SM, Emery SB, Hirst S. 2017. Use of spatially distributed time-integrated sediment sampling networks and distributed fine sediment modelling to inform catchment management. Journal of Environmental Management : 1–10. DOI: 10.1016/j.jenvman.2017.01.045 [online] Available from: http://dx.doi.org/10.1016/j.jenvman.2017.01.045

Peukert S, Griffith BA, Murray PJ, Macleod CJA, Brazier RE. 2014. Intensive management in grasslands causes diffuse water pollution at the farm scale. Journal of environmental quality **43** : 2009–23. DOI: 10.2134/jeq2014.04.0193 [online] Available from: http://apps.webofknowledge.com/full_record.do?product=UA&search_mode=MarkedList&qid=5&SID=X1GdoygYIDJf68Z2HEq&page=1&doc=2&colName=WOS

Pietroń J, Jarsjö J, Romanchenko AO, Chalov SR. 2015. Model analyses of the contribution of in-channel processes to sediment concentration hysteresis loops. Journal of Hydrology **527** : 576–589. DOI: 10.1016/j.jhydrol.2015.05.009 [online] Available from: http://www.sciencedirect.com/science/article/pii/S0022169415003583%5Cnhttp://linkinghub.elsevier.com/retrieve/pii/S0022169415003583

Poulenard J, Legout C, Némery J, Bramorski J, Navratil O, Douchin A, Fanget B, Perrette Y, Evrard O, Esteves M. 2012. Tracing sediment sources during floods using Diffuse Reflectance Infrared Fourier Transform Spectrometry (DRIFTS): A case study in a highly erosive mountainous catchment (Southern French Alps). Journal of Hydrology **414–415** : 452–462. DOI: 10.1016/j.jhydrol.2011.11.022 [online] Available from: http://linkinghub.elsevier.com/retrieve/pii/S0022169411008079 (Accessed 17 October 2014)

Poulenard J, Perrette Y, Fanget B, Quetin P, Trevisan D, Dorioz JM. 2009. Infrared spectroscopy tracing of sediment sources in a small rural watershed (French Alps). The Science of the total environment **407** : 2808–19. DOI: 10.1016/j.scitotenv.2008.12.049 [online] Available from: http://www.ncbi.nlm.nih.gov/pubmed/19176234 (Accessed 17 October 2014)

Pulley S, Collins AL. 2018. Tracing catchment fine sediment sources using the new

SIFT (SedIment Fingerprinting Tool) open source software. Science of the Total Environment **635** : 838–858. DOI: 10.1016/j.scitotenv.2018.04.126 [online] Available from: https://doi.org/10.1016/j.scitotenv.2018.04.126

Pulley S, Foster I, Antunes P. 2015. The uncertainties associated with sediment fingerprinting suspended and recently deposited fluvial sediment in the Nene river basin. Geomorphology **228** : 303–319. DOI: 10.1016/j.geomorph.2014.09.016 [online] Available from: http://linkinghub.elsevier.com/retrieve/pii/S0169555X14004917 (Accessed 7 January 2015)

Rovira A, Ibáñez C, Martín-Vide JP. 2015. Suspended sediment load at the lowermost Ebro River (Catalonia, Spain). Quaternary International **388** : 188–198. DOI: 10.1016/j.quaint.2015.05.035

Rügner H, Schwientek M, Egner M, Grathwohl P. 2014. Monitoring of event-based mobilization of hydrophobic pollutants in rivers: calibration of turbidity as a proxy for particle facilitated transport in field and laboratory. The Science of the total environment **490** : 191–8. DOI: 10.1016/j.scitotenv.2014.04.110 [online] Available from: http://www.ncbi.nlm.nih.gov/pubmed/24858216 (Accessed 22 September 2014)

Sear DA, Malcolm DN, Thorne CR. 2003. Guidebook for Applied Fluvial Geomorphology, R&D Technical Report FD1914 . London [online] Available from: http://www.waterbouw.tudelft.nl/fileadmin/Faculteit/CiTG/Over_de_faculteit/Afdelingen/Afdeling_Waterbouwkunde/sectie_waterbouwkunde/people/personal/gelder/publications/citations/doc/citatie86.pdf%5Cnhttp://www.river-conveyance.net/2_AES_UserGuide.pdf

Seeger M, Errea MP, Beguería S, Arnáez J, Martí C, García-Ruiz JM. 2004. Catchment soil moisture and rainfall characteristics as determinant factors for discharge/suspended sediment hysteretic loops in a small headwater catchment in the Spanish pyrenees. Journal of Hydrology **288** : 299–311. DOI: 10.1016/j.jhydrol.2003.10.012

Sherriff SC, Rowan JS, Fenton O, Jordan P, Melland AR, Mellander PE, Huallacháin D. 2016. Storm Event Suspended Sediment-Discharge Hysteresis and Controls in Agricultural Watersheds: Implications for Watershed Scale Sediment Management. Environmental Science and Technology **50** : 1769–1778. DOI: 10.1021/acs.est.5b04573

Smith HG, Dragovich D. 2009. Interpreting sediment delivery processes using suspended sediment-discharge hysteresis patterns from nested upland catchments, south-eastern Australia. Hydrological Processes **23** : 2416–2426. DOI: 10.1002/hyp [online] Available from: http://jamsb.austms.org.au/courses/CSC2408/semester3/resources/ldp/abs-guide.pdf

Sun L, Yan M, Cai Q, Fang H. 2015. Suspended sediment dynamics at different time scales in the Loushui River, south-central China. Catena **Published** DOI: 10.1016/j.catena.2015.02.014 [online] Available from: http://linkinghub.elsevier.com/retrieve/pii/S0341816215000569

Taylor KG, Owens PN. 2009. Sediments in urban river basins: a review of sediment–contaminant dynamics in an environmental system conditioned by human activities. Journal of Soils and Sediments **9** : 281–303. DOI: 10.1007/s11368-009-0103-z [online] Available from: http://link.springer.com/10.1007/s11368-009-0103-z (Accessed 14 October 2014)

Tena A, Vericat D, Batalla RJ. 2014. Suspended sediment dynamics during flushing flows in a large impounded river (the lower River Ebro). Journal of Soils and Sediments **14** : 2057–2069. DOI: 10.1007/s11368-014-0987-0 [online] Available from: http://link.springer.com/10.1007/s11368-014-0987-0 (Accessed 3 December 2014)

Tiecher T, Caner L, Minella JPG, Evrard O, Mondamert L, Labanowski J, Rheinheimer dos Santos D. 2016. Tracing Sediment Sources using Mid-Infrared Spectroscopy in Arvorezinha Catchment, Southern Brazil. Land Degradation & Development DOI: 10.1002/ldr.2690 [online] Available from: http://doi.wiley.com/10.1002/ldr.2690

Trimble SW, Mendel AC. 1995. The cow as a geomorphic agent--a critical review. Geomorphology **13** : 233–253.

Vale SS, Fuller IC, Procter JN, Basher LR, Smith IE. 2016. Characterization and quantification of suspended sediment sources to the Manawatu River, New Zealand. Science of The Total Environment **543** : 171–186. DOI: 10.1016/j.scitotenv.2015.11.003 [online] Available from: http://www.sciencedirect.com/science/article/pii/S0048969715309840

Vanmaercke M, Ardizzone F, Rossi M, Guzzetti F. 2016. Exploring the effects of seismicity on landslides and catchment sediment yield: An Italian case study. Geomorphology DOI: 10.1016/j.geomorph.2016.11.010 [online] Available from: http://linkinghub.elsevier.com/retrieve/pii/S0169555X16310698

Vercruysse K, Grabowski RC. 2018. Using source-specific models to test the impact of sediment source classification on sediment fingerprinting. Hydrological Processes : 3402–3415. DOI: 10.1002/hyp.13269

Vercruysse K, Grabowski RCRC, Rickson RJ. 2017. Suspended sediment transport dynamics in rivers: Multi-scale drivers of temporal variation. Earth-Science Reviews **166** : 38–52. DOI: 10.1016/j.earscirev.2016.12.016 [online] Available from: http://linkinghub.elsevier.com/retrieve/pii/S001282521630229X

Walling DE. 2013. The evolution of sediment source fingerprinting investigations in fluvial systems. Journal of Soils and Sediments **13** : 1658–1675. DOI: 10.1007/s11368-013-0767-2 [online] Available from: http://link.springer.com/10.1007/s11368-013-0767-2 (Accessed 4 November 2014)

Walling DE, Owens PN, Carter J, Leeks GJL, Lewis S, Meharg AA, Wright J. 2003a. Storage of sediment-associated nutrients and contaminants in river channel and floodplain systems. Applied Geochemistry **18** : 195–220. DOI: 10.1016/S0883-2927(02)00121-X

Walling, Owens PN, Foster IDL, Lees JA. 2003b. Changes in the fine sediment

dynamics of the Ouse and Tweed basins in the UK over the last 100-150 years. Hydrological Processes **17** : 3245–3269. DOI: 10.1002/hyp.1385

Williams GP. 1989. Sediment concentration versus water discharge during single hydrologic events in rivers. Journal of Hydrology **111** : 89–106. DOI: 10.1016/0022-1694(89)90254-0

Wohl E. 2015. Legacy effects on sediments in river corridors. Earth-Science Reviews **147** : 30–53. DOI: 10.1016/j.earscirev.2015.05.001 [online] Available from: http://dx.doi.org/10.1016/j.earscirev.2015.05.001

Wold S, Sjostrom M, Eriksson L. 2001. PLS-regression : a basic tool of chemometrics. Chemometrics and Intelligent Laboratory Systems **58** : 109–130.

Zeiger S, Hubbart JA. 2016. Quantifying suspended sediment flux in a mixed-land-use urbanizing watershed using a nested-scale study design. Science of the Total Environment **542** : 315–323. DOI: 10.1016/j.scitotenv.2015.10.096 [online] Available from: http://dx.doi.org/10.1016/j.scitotenv.2015.10.096

Zimmermann A, Francke T, Elsenbeer H. 2012. Forests and erosion: Insights from a study of suspended-sediment dynamics in an overland flow-prone rainforest catchment. Journal of Hydrology **428–429** : 170–181. DOI: 10.1016/j.jhydrol.2012.01.039 [online] Available from: http://dx.doi.org/10.1016/j.jhydrol.2012.01.039